5296 *Macromolecules* **2009**, *42*, 5296–5302
DOI: 10.1021/ma900707p

Macromolecules
ARTICLE

Methodology for Quantitative Measurements of Multilayer Polymer Thin Films with IR Spectroscopic Ellipsometry

Shuhui Kang, Vivek M. Prabhu, Christopher L. Soles, Eric K. Lin, and Wen-li Wu*

Polymers Division, National Institute of Standards and Technology, 100 Bureau Dr, Gaithersburg, Maryland 20899

Received April 1, 2009; Revised Manuscript Received June 15, 2009

ABSTRACT: A new methodology to quantify the sensitivity and resolution of infrared spectroscopic ellipsometry (IRSE) measurements was developed for probing the depth profile of composition in thin polymer films. A multilayer system comprised of sub-100 nm films of poly(4-hydroxystyrene) on top of poly (methyladamantyl methacrylate) was used as a model test structure for our IRSE measurements of bilayer film thickness and composition profile. The IRSE results are further validated by comparing to high-resolution neutron reflectivity results also from these samples. We demonstrated that the substrate type, incident angle, and specific spectral band regions strongly influence the sensitivity of IRSE; a judicious choice of measurement variables and infrared spectral regions can substantially improve the measurement in terms of sensitivity. Most strikingly, an incidence at the Brewster angle of the substrate does not lend to the maximum sensitivity. Discussions of the origin of these findings and metrics are provided.

1. Introduction

Infrared spectroscopic ellipsometry (IRSE) or infrared variable angle spectroscopic ellipsometry (IR-VASE) is used extensively to characterize semiconductor and organic thin films.[1−4] IRSE is widely applied to quantify the molecular orientation of organic and inorganic monolayers because the signal-to-noise ratio in the measurement is larger than that from traditional Fourier transform infrared spectroscopy.[5−11] Recently, the use of IRSE was evaluated to study polymer interfaces and interdiffusion as a complementary method to neutron reflectivity (NR) and X-ray reflectivity (XR).[12−15] IRSE was selected because most polymer materials possess very strong and distinct absorption bands, known as "fingerprints", in the mid-IR spectral region. These absorption bands, corresponding to the imaginary part of the refractive index, can provide large optical contrast among different polymer species. This feature provides IRSE a unique advantage because most organic polymer systems have similar electron densities or neutron scattering length densities and cannot be distinguished in XR or NR measurements. Ellipsometry in the visible and ultraviolet regions encounters a similar lack of contrast because the refractive indices of polymers are similar.

For polymer interfaces, Duckworth et al.[12] demonstrated that the interdiffusion between two polymers upon annealing can be detected with IRSE. Hinrichs et al.[13,14,16] showed that the interdiffusion in a bilayer film induced by annealing could be modeled with a three-layer model. Further, Nikonenko et al.[15] used IRSE to investigate the annealing induced interaction in thin polymeric double layers. However, most of the previous work has been qualitative or semiquantitative because of either a lack of well-defined optical constants of the studied materials or inadequate sensitivity. Using IRSE to study thin polymer films is challenging because the IR wavelength (≈5−10 μm) is much larger than the thicknesses of the thin films and the interfacial width. Therefore, sensitivity is an intrinsic issue, and it merits further development before IRSE can provide quantitative measurements of polymer films. In this work, we introduced a sensitivity parameter to facilitate the optimization of the experimental parameters used in IRSE studies of polymer bilayers.

*Corresponding author: e-mail wenli@nist.gov, tel 301-975-6839, fax 301-975-3928.

2. Experimental Section[21]

2.1. Sample Preparation. A series of single-layer and bilayer films were prepared by spin-coating poly(4-hydroxystyrene) (PHOSt) (mass-average relative molecular mass M_w = 120 000 g mol^{-1}) and poly(methyladamantyl methacrylate) (PMAdMA) (mass-average relative molecular mass M_w = 8800 g mol^{-1}) from organic solvents onto silicon wafers followed by baking at 130 °C for 60 s. Bilayer films are prepared by spin-coating a cold cyclohexanone solution of PHOSt on a precoated and dried PMAdMA layer film. Cold cyclohexanone resulted in limited dissolution and interdiffusion of the bottom PMAdMA layer at a spinning speed 2000 rpm (209 rad/s). The interfacial width between PMAdMA and PHOSt was found to be ≈10 nm as determined by NR; the details will be discussed later.

These polymer materials are widely used as photoresists and possess strong and well-separated absorption bands that provide the needed IRSE contrast. In addition, their neutron scattering contrast is sufficient for NR characterization, and a direct comparison of the composition depth profile between the two techniques is available.

All thin films were prepared on highly doped single side polished silicon wafers to reduce the backside reflection that occurs with double-side polished wafers. The wafers were precleaned in a hydrofluoric acid (HF) solution to remove the native oxide followed by ultraviolet (UV)/ozone treatment for 2 min to grow a ≈1 nm oxide layer. Because of the moderate reflectivity of silicon and the low sensitivity of the deuterated triglycine sulfate (DTGS) detector used in this work, the IRSE results obtained with silicon as the substrate usually contain significant noise that makes thin film measurements very difficult, especially when film thickness is less than 100 nm. To overcome this problem, polymer films were also prepared on highly reflective gold-coated silicon wafers. The gold of 100 nm thick was evaporated upon silicon wafers at the National

 Published on Web 07/02/2009

Institute of Standards and Technology (NIST, Gaithersburg, MD). A joint fit of the IRSE results from polymer films coated on these two different substrates provides a reliable approach to accurately determine the optical constants of the polymer films.

2.2. Instrumentation. *2.2.1. Infrared Variable Angle Spectroscopic Ellipsometer (IR-VASE).* The IRSE used in the measurement was manufactured by J.A. Woollam Co., Inc., with a nominal precision of incident angle of 0.005°. A standard globar IR source provides a spectral coverage between 600 and 6000 cm^{-1}. The angular divergence or the opening angle of the IR beam is ±0.8° or 1.6 ° fwhm at 75° incident angle. This value was determined by rocking a silicon wafer at the sample position with the detector staying fixed at 150°. The rotating compensator configuration provides a high accuracy in the measurement of the phase angle (Δ) at any incidence angle. This configuration is different from the more common ellipsometer that uses a rotating polarizer/analyzer approach that is difficult to measure Δ near the Brewster angle.[17] A DTGS detector is employed to record the IR spectra at room temperature with a resolution of 8 cm^{-1}. Usually three incident angles—65°, 75°, and 85°—are used with multiple scans to reduce the noise level. The typical running time for each sample is 8−12 h. It is noteworthy that the angle of 75° is above the silicon Brewter angle over the spectrum range used in this work even one considers the open angle of ±0.8°.

2.2.2. X-ray Reflectivity and Neutron Reflectivity. X-ray reflectivity measurements were performed using a modified high-resolution X-ray diffractometer with Cu Kα radiation. Neutron reflectivity measurements were performed at the Center for Neutron Research on the NG-7 reflectometer at the NIST. The wavelength (λ) of the neutron beam is 4.768 Å with a wavelength spread (Δλ/λ) of 0.025.

2.3. Modeling and Simulation. The quantities measured in ellipsometry are Ψ and Δ and are defined as

$$\rho = \frac{R_p}{R_s} = \tan \Psi e^{i\Delta} \quad (1)$$

where ρ is the ratio of the Fresnel reflection coefficients R_p and R_s for the p- and s-polarized light, respectively. From these two quantities, one deduces unknown parameters including film thickness (*d*), the refractive index (*n*), and the absorption coefficient (*k*) of the thin film upon a substrate of known *n* and *k*.

In order to determine the polymer multilayer thickness and composition from Ψ and Δ, we need to predetermine the optical constants *n* and *k* for each pure polymer component. This measurement is performed most accurately by using single-layer films on multiple well-defined substrates.[18] In this work, Si and Au surfaces were used to obtain high-precision measurements of *n* and *k*. X-ray reflectivity was used to independently measure the film thickness with angstrom resolution. IRSE over the transparent regions can be used to determine film thickness. For most nonconductive polymers there is an IR-transparent spectral window around 4000−6000 cm^{-1}, over which we can assume the absorption or *k* is zero. For a nonabsorbing single layer film, the Cauchy model

$$n(\lambda) = n_0 + \frac{A}{\lambda^2} + \frac{B}{\lambda^4} \quad (2)$$

is used to relate refractive index to wavelength. The three coefficients n_0, *A*, and *B* and the film thickness can all be determined with the IRSE data over the IR transparent region. To improve the precision of film thickness, we prepared films on both Si and Au substrates and performed a joint fit of the IRSE data from two substrates assuming the coefficients do not change from substrate to substrate.

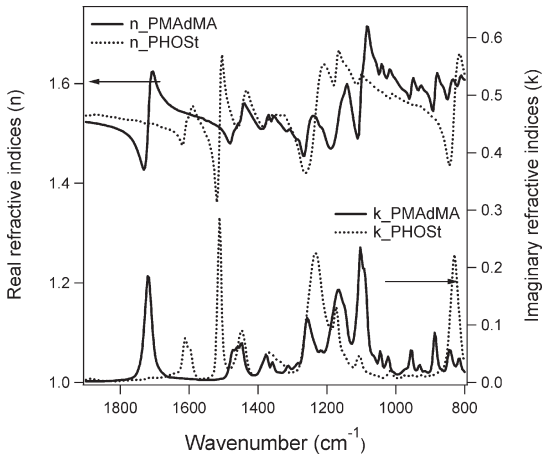

Figure 1. Optical constants *n* and *k* fitted from IRSE spectra for single-layer film samples of PHOSt and PMAdMA, respectively.

Scheme 1. A Bilayer Film Changes to a Single-Layer Film through Virtual Interdiffusion[a]

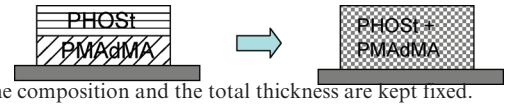

[a] The composition and the total thickness are kept fixed.

With a known thickness, the optical constants of a polymer can be obtained from the Ψ and Δ spectra of a single layer film over the entire wavenumber range covered by IRSE through joint fitting. All the data in the spectra region are fitted simultaneously with the iterative Marquardt−Levenberg fitting algorithm. The modeling and parameter fitting are made by minimizing the root-mean-square error (MSE) defined as follows:

$$\mathrm{MSE} = \sqrt{\frac{1}{2N-M}\sum_{i=1}^{N}\left[\left(\frac{\psi_i^{\mathrm{mod}}-\psi_i^{\mathrm{exp}}}{\sigma_{\psi,i}^{\mathrm{exp}}}\right)^2+\left(\frac{\Delta_i^{\mathrm{mod}}-\Delta_i^{\mathrm{exp}}}{\sigma_{\Delta,i}^{\mathrm{exp}}}\right)^2\right]} \quad (3)$$

Here *N* equals the number of data points (ψ_i and Δ_i pairs) in the chosen spectral band and *M* are the number of fitting parameters, while $\sigma_{\psi,i}^{\mathrm{exp}}$ and $\sigma_{\Delta,i}^{\mathrm{exp}}$ are the standard deviation for the measured ψ_i and Δ_i, respectively. The fitting error of parameter *i* is calculated by $\mathrm{error}_i = 1.65\mathrm{MSE}(C_{ii})^{1/2}$, where the C_{ii} is the *i*th diagonal element of the covariance matrix about fitting parameters. The coefficient 1.65 corresponds to a 90% confidence interval.

3. Results and Discussion

3.1. Polymer Optical Constants. The single-layer film thickness measured from IRSE in the IR-transparent region is consistent with the XR results to within 1−2 nm. The *n* values from IRSE for two well-known polymers, PMMA and PS, at 2 μm wavelength are 1.486 and 1.563, respectively, which are comparable to published literature values in the visible region of 1.492 and 1.590, respectively, at a 0.589 μm wavelength. On the basis of the simple dispersion consideration, one expects a smaller refractive index at longer wavelengths, which is consistent with these results

The real and imaginary parts of the refractive index, $N = n + ik$, obtained for PMAdMA and PHOSt via a joint fit of data from two substrates (Si and Au) are shown in Figure 1. There are several band regions with unique absorption for one polymer, but not the other, such as 1720 cm^{-1} for the C=O stretching of PMAdMA and 1600 and 1510 cm^{-1} for

the C=C stretching of PHOSt. Therefore, these absorption bands provide high sensitivity for probing the bilayer structure. Alternatively, absorption regions that are common to PHOSt and PMAdMA include 1220 cm^{-1} for the C−O stretching and 830 cm^{-1} for the C−C stretching. However, they appear at significantly different intensities and may also enhance the bilayer analysis.

The accuracy of optical constants is critical for accurate measurements of the polymer−polymer interface study and merits further discussion. The real part and the imaginary part of the refractive indices or the dielectric constants $\varepsilon = \varepsilon_1 + i\varepsilon_2 = (n + ik)^2$ are related via the following Kramers−Kronig (K−K) relation

$$\varepsilon_1(\nu) = 1 + \frac{2}{\pi} P \int_0^\infty \frac{\nu' \varepsilon_2(\nu')}{\nu'^2 - \nu^2} \, d\nu' \tag{4}$$

where P is the principal value of the integral and ν is the frequency or the wavenumber. Figure 2 shows a comparison between the measured ε_1 (symbols) and the calculated ε_1 (lines) by applying the K−K relations to the measured ε_2 for PMAdMA and PHOSt, respectively. The numerical integration of eq 4 was conducted over the frequency range of 600−6000 cm^{-1}. The excellent agreement between the calculated ε_1 and the measured ε_1 demonstrate that the optical constants follow the K−K relation for both polymers.

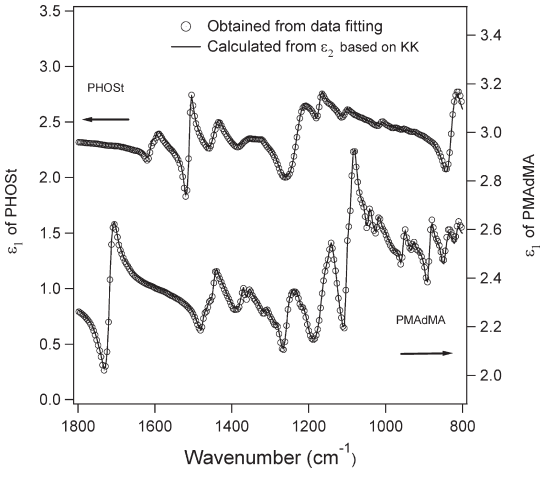

Figure 2. Measured ε_1 (single layer) vs calculated ε_1 from ε_2 based on K−K relations for PHOSt and PMAdMA.

To further verify the optical constants from IRSE measurements, the absorption coefficients (A) are measured by transmission IR, and the result can be compared with the imaginary part of the refractive index k through the relation $A = 4\pi k/\lambda$. Figure 3 shows the comparison of the absorption coefficients of PMAdMA and PHOSt calculated from the k values and those measured with transmission FTIR. The reasonable agreement over the entire spectroscopic region indicates that optical constants based on IRSE are unbiased with good accuracy.

3.2. Sensitivity of Polymer Multilayers. The main objective of this work is to evaluate the sensitivity of IRSE for measurements of the interface between two polymer films. To facilitate the discussion, we define a sensitivity parameter (S) in eq 5 at each wavenumber as the sum of the square of changes in Ψ and Δ after a virtual interdiffusion process that changes a bilayer film with a sharp interface into one with a uniform composition. Both the total thickness and the composition are conserved in this virtual process (Scheme 1). The calculation of the optical constants in the mixing layer is based on the Bruggeman effective media approximation, and the domain shape in the mixture is assumed to be spherical and isotropic with depolarization ratio equal to 1/3.[19]

$$S = \sqrt{\delta\psi^2 + \delta\Delta^2} \tag{5}$$

We also define a contrast parameter (C) as the root-mean-square of the difference in n and k between these two polymers.

$$C = \sqrt{\delta n^2 + \delta k^2} \tag{6}$$

The model bilayer studied in this work is PHOSt on top of PMADMA. Figure 4 shows a simulated result between the sensitivity and the contrast as a function of wavenumber with a 75° incident angle that is above but close to the substrate Si's Brewster angle of 73.7°−73.9° for the spectral region 600−6000 cm^{-1} used in this work. It can be seen that both the contrast and sensitivity are enhanced near the IR absorption region.

The relation between the sensitivity and the contrast from the above figure is plotted in Figure 5, and the result indicates that high contrast leads to high sensitivity as expected. The

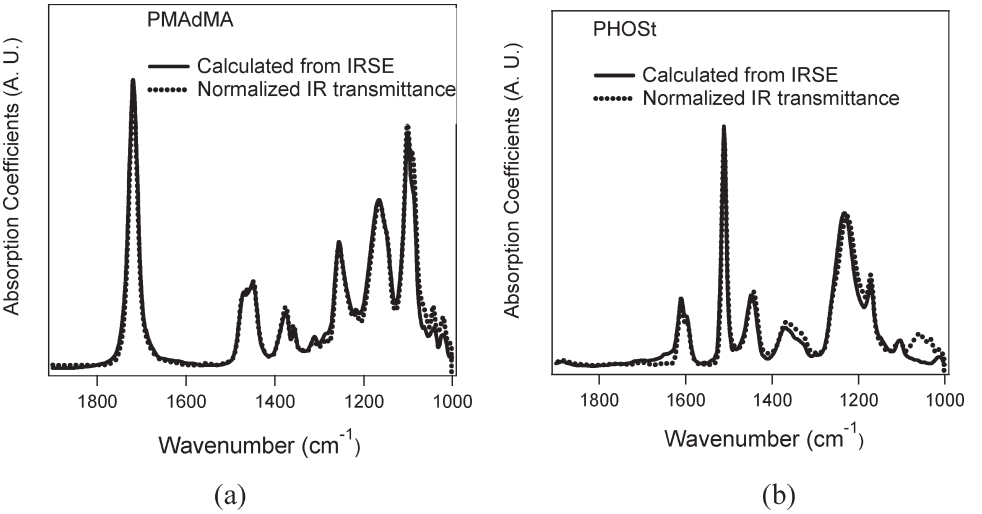

Figure 3. IR absorption coefficients calculated from the fitted imaginary part of refractive index k with IRSE vs directly measured with transmission FTIR (films compressed on CaF_2 disks) normalized by the strongest bands for PMAdMA (a) and PHOSt (b).

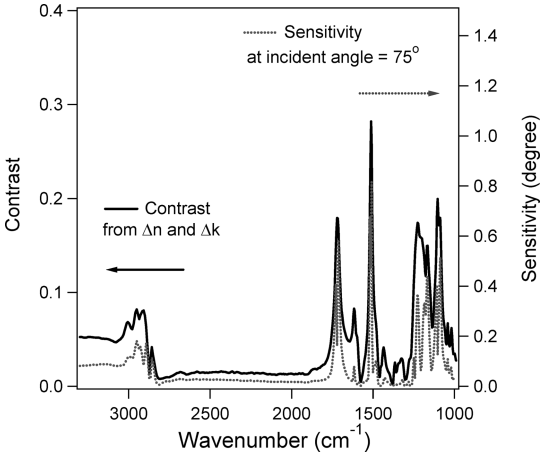

Figure 4. Calculated sensitivity and contrast as a function of wavenumber. The sensitivity is calculated based on a virtual physical process in which a PHOSt (100 nm)/PMAdMA(100 nm) bilayer on Si substrate changes to a 200 nm uniform single-layer film.

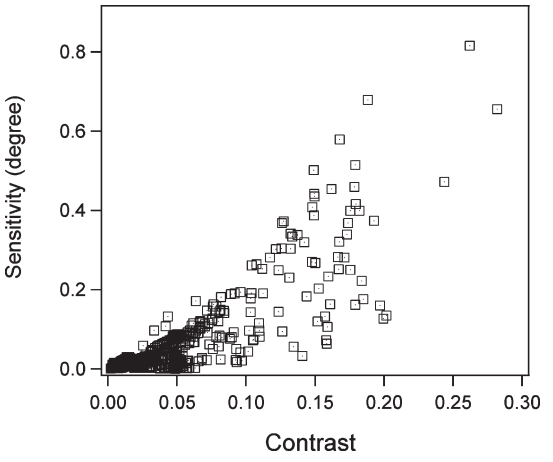

Figure 5. Simulated sensitivity and the contrast of PMADMA/PHOSt bilayers at an incident angle of 75°.

widespread of the data suggests that the sensitivity depends on other factors in addition to contrast.

The calculated sensitivity at an incident angle of 75° in the mid-IR region of 1000−1800 cm^{-1} is given in Figure 6 together with the absorption bands of each polymer. It can be seen that high sensitivity exists in the wavenumber range where only one of the polymers has strong IR absorption, such as near 1720 and 1510 cm^{-1}, while the sensitivity around bands near 1450 and 1360 cm^{-1} are low because these bands from the two polymers are overlapped and with similar intensity. However, an unanticipated dip in sensitivity appears near the peak of certain IR absorption bands, for example at 1720 cm^{-1}.

To understand the apparent loss in sensitivity, we simulated the sensitivity at an incident angle of 65° and did not see such a dip (Figure 7a). Therefore, the sensitivity does not always reach a maximum near the Brewster angle, contrary to the conventional wisdom established for ellipsometer measurements of single-layer thin film supported on substrate.[20] Our results below further highlight the complexity in identifying the experimental configuration that optimizes the sensitivity of IRSE. The sensitivity at two wavenumbers, 1720 and 1712 cm^{-1}, were calculated as a function of incident angle, and the results are given in Figure 7b. It shows that there is indeed a dip in sensitivity around the substrate

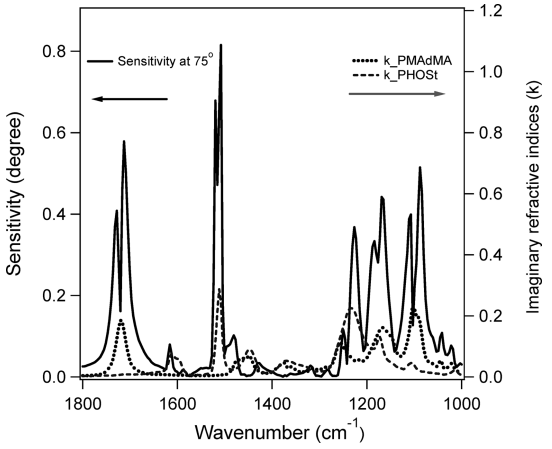

Figure 6. IR absorption bands of PHOSt, PMAdMA, and the calculated sensitivity based on a virtual physical process in which a PHOSt (100 nm)/PMAdMA(100 nm) bilayer on Si substrate changes to a 200 nm uniform single-layer film.

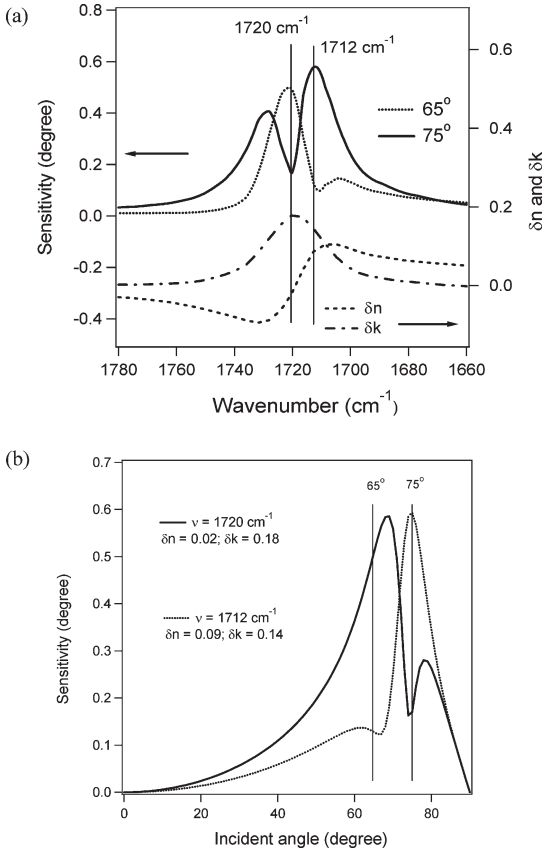

Figure 7. (a) Upper: sensitivity calculated for two different angle 65° and 75° around C═O band region. Lower: difference in the real and the imaginary parts of refractive indices between PMAdMA and PHOSt around C═O band region. (b) Calculated sensitivity vs incident angle at 1720 cm^{-1} band where the $\delta n \approx 0$ or $\ll \delta\kappa$ and at 1712 cm^{-1} band where the $\delta n \approx \delta\kappa$ between the two polymers.

Brewster angle, and the sensitivity reaches a maximum around 70° at 1720 cm^{-1} whereas for 1712 cm^{-1} the sensitivity reaches a maximum at 74° and a minimum near 65°. The reason underlining this sensitivity dip at peak position is not clear but could be related to the fact that the difference in real part of refractive indices is close to zero ($\delta n \approx 0$) or much smaller than that in imaginary part of refractive indices ($\delta n \ll \delta k$) between two polymers.

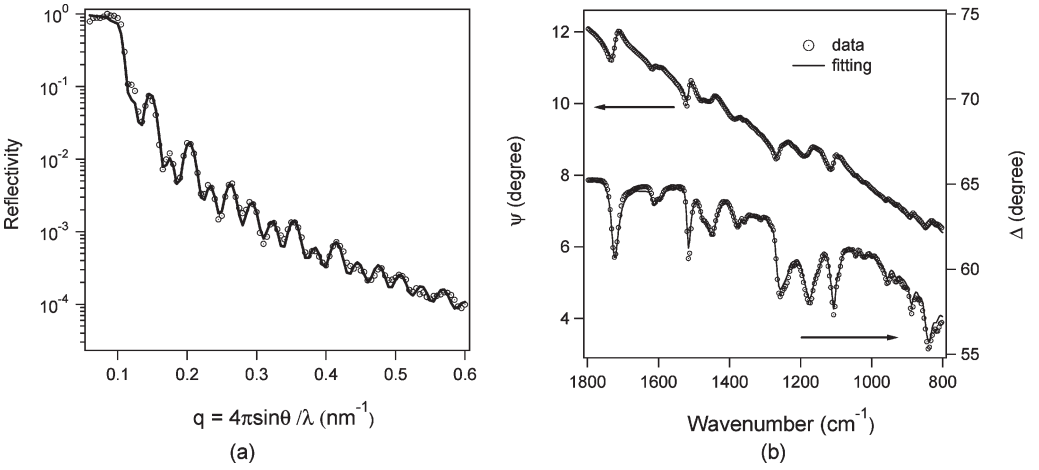

Figure 8. (a) NR data (dots) and its fit (solid lines) (b) the measured (dots) and fit (solid lines) of Ψ and Δ from a PHOSt/PMAdMA bilayer film measured at an incident angle 75°.

Table 1. Bilayer Film Structure in Terms of the Thickness of Individual Layer Thickness (in Å) Determined from NR and IRSE

	top layer (PHOSt) [nm]	interfacial layer (50:50 mix) [nm]	bottom layer (PMAdMA) [nm]	experimental conditions
NR	85 ± 1	8 ± 1[a]	116 ± 1	
IRSE	67 ± 16	0 ± 31[b]	138 ± 16	spectral region: 800−4000 cm^{-1}; incident angle: 65°, 75°, 85°

[a] The uncertainty is corresponding to 90% confidence interval. [b] The first number is the optimum central value fitted, and the second number is the fitting error corresponding to 90% confidence interval. It should be noted that thickness should be non-negative by definition. If the lower limit of a thickness value is less than zero, it should be treated as zero.

Table 2. Model Fitted Layer Thickness and Uncertainty

			fitted layer thickness and uncertainty			
contrast	band region (cm^{-1})	vibration	top layer (PHOSt)	intermediate (50:50 mix)	bottom layer (PMAdMA)	fitted MSE
high	1400−1800	ν(C=O), ν(C=C)	71 ± 8	13 ± 17	121 ± 9	0.48
medium/high	1000−1400	ν(C−O), δ(C−H)	66 ± 23	0 ± 44	139 ± 21	0.92
low	2800−3200	ν(C−H), ν(O−H)	73 ± 51	0 ± 99	132 ± 49	0.47
~zero	2000−2400	none	22 ± 772	0 ± 1510	183 ± 746	0.42

It should be noted that our simulated results given in Figures 6 and 7 do not provide general guidelines of selecting experimental settings to maximize the IRSE sensitivity for bilayer interface measurements. Instead, the results demonstrate the intricacy of the IRSE measurement in terms of the dependence of sensitivity on experimental parameters.

3.3. Characterization of PHOSt/PMAdMA Bilayer Film Structure. With the optical constants of both PHOSt and PMAdMA obtained from single-layer films, we now return to the bilayer structure measurement. Here a PHOSt/PMAdMA bilayer film sample on Si substrate was measured by both NR and IRSE, and the results were analyzed with a trilayer model (PHOSt, PMAdMA layers and an interfacial layer). The experimental data and the fits are shown in Figure 8 and Table 1.

The uncertainty in the IRSE measurements is larger than that from neutron reflectivity measurements. For example, IRSE finds the fitted thickness of the interfacial layer as zero with an uncertainty of 31 nm. The IRSE results listed in Table 1, however, are obtained by fitting the entire wavenumber region between 800 and 4000 cm^{-1}. As described previously, this result can be improved by choosing data from the high-contrast regions. This process was performed over several specific regions with the results tabulated in Table 2.

It can be seen that the fit parameter error is dictated by the contrast rather than the MSE, although MSE reflects how close the model is to the data. For example, the MSE at the 2000−2400 cm^{-1} region is smaller than at 1400−1800 cm^{-1}, but the fitting error is much larger. This error arises because the sensitivity at 2000−2400 cm^{-1} is much lower due to a low contrast. This study tells us that a proper choice of band region with higher contrast greatly improves the sensitivity and reduces the fit uncertainty.

It should be mentioned that the MSE is significantly larger in the 1000−1400 cm^{-1} region than other regions. This is due to the fact that the optical constants are less accurate between 1000 and 1200 cm^{-1} (see Figure 3) because this band region is influenced by the stretching vibration of Si−O associated with silicon substrates. This fact reflects the importance of accurate optical constants as demonstrated by the simulation results.

The above results demonstrate that by rationally selecting band regions with high contrast the fitting uncertainty can be greatly reduced. In addition, the effect of incident angle on IRSE sensitivity is explored as follows. Table 3 lists the model fitted multilayer film thickness and uncertainty for various incident angle and their combinations. The sensitivity for each angle can be qualitatively estimated from Figure 7b.

Table 3 shows that the sensitivity and the resulted fit uncertainty at 65° are greater or at least not lower than at 75°. The sensitivity at 85° is much lower than other two angles. Further, a combination of 65° and 75° enhances the sensitivity by reducing the fit uncertainty.

Table 3. IRSE Model Fits over the Spectral Region 1400−1800 cm^{-1}

		fitted layer thickness and uncertainty			
sensitivity	incident angles (deg)	top layer (PHOSt)	intermediate (50:50 mix)	bottom layer (PMAdMA)	fitted MSE
high	65	72 ± 8	11 ± 16	122 ± 8	0.35
high	75	74 ± 9	6 ± 17	124 ± 9	0.44
low	85	75 ± 25	4 ± 49	125 ± 25	0.55
high + high	65, 75	73 ± 6	8 ± 13	124 ± 7	0.43
high + low	75, 85	74 ± 9	6 ± 18	125 ± 10	0.50
high + low	65, 85	73 ± 10	9 ± 20	123 ± 10	0.49
high + high + low	65, 75, 85	74 ± 7	7 ± 14	124 ± 7	0.48

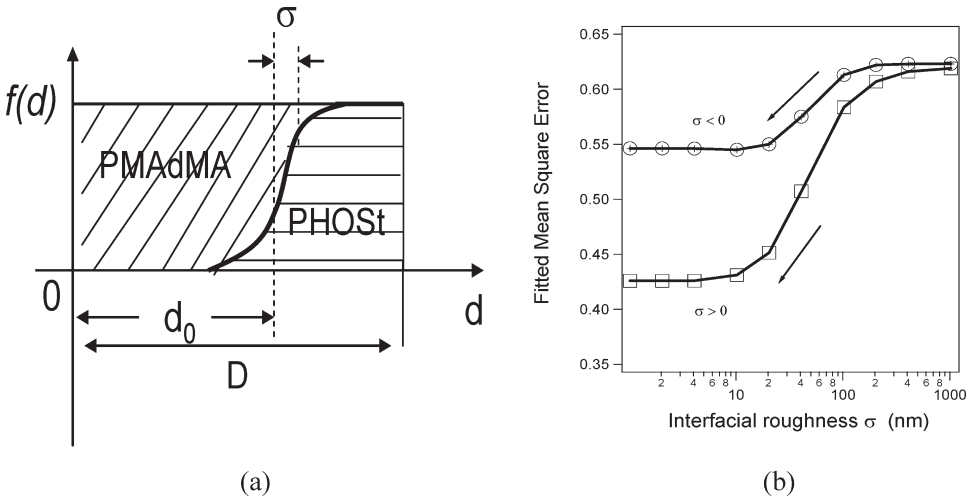

(a) (b)

Figure 9. (a) Layout of bilayer and interfacial structure. (b) Fitted MSE for various interfacial width. The lines are drawn to guide the eye.

Therefore, by choosing an appropriate combination of band regions and incident angles the uncertainty in the fitted polymer multilayer structure was significantly decreased; from (67 ± 16) nm/(0 ± 31) nm/(138 ± 16) nm to (73 ± 6) nm/(8 ± 13) nm/(124 ± 7) nm as the top/interface/bottom thickness. The latter result is also quite close to the layer structure determined by neutron reflectivity, 85 nm/8 nm/116 nm.

It should be noted that the same bilayer samples could also be prepared on Au substrate. However, a simulation study shows that the sensitivity with Au substrate is much lower than with Si substrate at the same conditions although the noise level could be lower due to higher reflectivity; e.g., a calculation has shown that the average sensitivity between 1400 and 1800 cm^{-1} spectral region on Au substrate for 100 nm PMAdMA/100 nm PHOSt bilayer is about 0.5 times that on Si substrate at a 65° incident angle. The reason could be related to the large imaginary part of refractive indices in Au which results in the reflectivity at s-polarization (R_s) very close to 1, therefore insensitive to the polymers on it. Thus, we did not use bilayer samples prepared on Au substrates. Additionally, since the three fitting parameters—thicknesses of top layer/interface/bottom layer—are not identical between samples, a joint fitting of multisamples with Si and Au substrate was not expected to reduce the uncertainty in the measurement.

3.4. Characterization of PHOSt/PMAdMA Multilayer Layout. The above discussion focuses on the bilayer structure, especially on the interface width and its uncertainty deduced from IRSE data. The general layout of the PHOSt/PMAdMA bilayers, i.e., PHOSt on top of PMAdMA which is in contact with the substrate, is given based on our sample preparation procedure. However, can IRSE discern an unknown bilayer layout? To facilitate the fitting, we choose a sigmoid function to describe the local concentration of PHOSt as a function of the depth z.

$$f(z) = \frac{1}{1+e^{(d_0 - z)/\sigma}} \quad (7)$$

where z is the distance from the substrate and d_0 and σ denote the thickness of the bottom layer and the interfacial width, respectively (Figure 9a). Note that σ can be either positive or negative; a positive σ gives rise to a small value of $f(z)$ at $z = 0$ and near unity at $z \gg d_0$. This type of bilayer layout with the PHOSt concentration approaching zero near the substrate and unity near the top surface is depicted in Figure 9a and represents the bilayer layout used in this work. A negative σ depicts the structure that PHOSt concentration reaches a maximum at $z = 0$ and decrease as z gets larger, i.e., a reverse bilayer layout. A discretization of σ from a large positive value to near zero (positive number) then from near zero (negative number) to a large negative value simulates all cases including from a very broad interface to a sharp interface with both normal layout and reverse layout.

Figure 9b shows the fitted MSE at various values of σ ranging from +1000 to −1000 nm (incident angle = 65° and 75°; fitting spectral region: 1400−1800 cm^{-1}). In general, MSE decreases as the interfacial roughness parameter σ decreases and reaches a plateau after σ becomes 10 nm or less. It is noteworthy that the MSE for normal layout ($\sigma > 0$) is always smaller than that of the reverse layout ($\sigma < 0$) at any given σ value. The above results indicate that IRSE is capable of identifying the correct bilayer layout. The resultant interfacial width is near 10 nm or less and is consistent with the data from the NR measurement. Moreover, it reveals that 10 nm is the resolution limit of IRSE to quantify interface width for the present case of a PMAdMA/PHOSt bilayer.

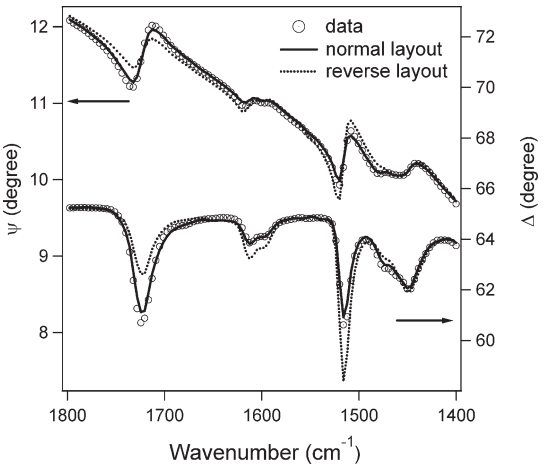

Figure 10. Simulated IRSE spectra for normal layout and reverse layout compared with data at incident angle 75°.

Figure 10 shows the simulated the Ψ and Δ spectra corresponding to normal layout structure and reverse layout structure. Obviously, the normal layout hypothesis agrees with the data much better than the reverse layout hypothesis particularly at the feature band regions around where there are maximum contrasts. Thus, the MSE difference in Figure 9b reflects the degree of discrepancy between the hypothesized structure and the real structure.

It is noteworthy that the hydrogen bond formation between the C═O in PMAdMA and the OH in PHOSt inside the interfacial region will result in changes in carbonyl band shapes. However, such a change in band shape is hardly discernible in Figure 10; the fit between the IRSE data and the normal layout model is satisfactory over the entire wavenumbers. The reason maybe that the volume fraction of the interfacial region only constitutes ~5% of the bilayer sample based on the neutron reflectivity result given in Table 1. In this case the total amount of H-bond formation may be very limited.

4. Conclusion

IRSE provides a unique methodology to characterize multilayer structures through the use of the absorption fingerprint regions and index differences between constituent films. To quantitatively evaluate the effect of experimental parameters including wavenumber regions and incident angle on the performance of IRSE, we chose a model bilayer structure on top of a silicon substrate and devised a methodology invoking the definition of sensitivity and contrast parameters. We demonstrated that the IRSE sensitivity can be improved by selecting the appropriate incident angle and absorption band regions. In general, only the high-contrast absorption regions, whereby strong and mutually exclusive IR bands, should be included in model fitting. For the present case study of PHOSt/PMAdMA bilayer on silicon with a 200 nm total film thickness, the incident angle near the Brewster angle of the substrate at 74° exhibited an unexpected drop in sensitivity near the peak wavenumber region of certain absorption bands. This type of drop in sensitivity disappeared at an incident angle of 65°. Therefore, the conventional approach to characterize thin films by ellipsometry at the substrate Brewster angle does not necessarily provide the highest sensitivity when considering multilayered organic films with absorption contrast. With this sensitivity and contrast parameter approach, we further demonstrated that the sequence of film stacking can be determined by IRSE. As compared with previous work, this study provides a quantitative and accurate characterization protocol that can be applied to other polymer or organic thin film systems.

The precise knowledge of the optical constant of the constituent films is a prerequisite for multilayer film characterization using IRSE. In this work, we demonstrated the use of a combination of neutron reflectivity and IRSE for determining the optical constant of a constituent film; with the film thickness value provided by neutron reflectivity a joint fit of the IRSE results from two different substrates yield high-quality data of both n and k. The k value so obtained is consistent with that from a direct transmission IR measurement.

References and Notes

(1) Gravalidis, C.; Logothetidis, S.; Hatziaras, N.; Laskarakis, A.; Tsiaoussis, I.; Frangis, N. *Appl. Surf. Sci.* **2006**, *253* (1), 385–388.
(2) Intelmann, C. M.; Hinrichs, K.; Syritski, V.; Yang, F.; Rappich, J. *Jpn. J. Appl. Phys.* **2008**, *47* (1), 554–557.
(3) Intelmann, C. M.; Syritski, V.; Tsankov, D.; Hinrichs, K.; Rappich, J. *Electrochim. Acta* **2008**, *53* (11), 4046–4050.
(4) Stenger, I.; Gallas, B.; Siozade, L.; Fisson, S.; Vuye, G.; Chenot, S.; Rivory, J. *Physica E* **2007**, *38* (1−2), 176–180.
(5) Hu, Z. G.; Prunici, P.; Patzner, P.; Hess, P. *J. Phys. Chem. B* **2006**, *110* (30), 14824–14831.
(6) Hu, Z. G.; Hess, P. *J. Vac. Sci. Technol. A* **2007**, *25* (3), 601–606.
(7) Laskarakis, A.; Logothetidis, S. *J. Appl. Phys.* **2006**, *99* (6), 066101_1–066101_3.
(8) Laskarakis, A.; Logothetidis, S. *Appl. Surf. Sci.* **2006**, *253* (1), 52–56.
(9) Roodenko, K.; Rappich, J.; Gensch, M.; Esser, N.; Hinrichs, K. *Appl. Phys. A: Mater. Sci. Process.* **2008**, *90* (1), 175–178.
(10) Hinrichs, K.; Gensch, M.; Roseler, A.; Esser, N. *J. Phys.: Condens. Matter* **2004**, *16* (39), S4335–S4343.
(11) Meuse, C. W. *Langmuir* **2000**, *16* (24), 9483–9487.
(12) Duckworth, P.; Richardson, H.; Carelli, C.; Keddie, J. L. *Surf. Interface Anal.* **2004**, *36*, 33–41.
(13) Hinrichs, K.; Gensch, M.; Nikonenko, N. A.; Pionteck, J.; Eichhorn, K. J. *Macromol. Symp.* **2005**, *230*, 26–32.
(14) Hinrichs, K.; Gensch, M.; Esser, N. *Appl. Spectrosc.* **2005**, *59* (11), 272A–282A.
(15) Nikonenko, N. A.; Hinrichs, K.; Korte, E. H.; Pionteck, J.; Eichhorn, K. J. *Macromolecules* **2004**, *37* (23), 8661–8667.
(16) Hinrichs, K.; Roseler, A.; Gensch, M.; Korte, E. H. *Thin Solid Films* **2004**, *455*, 266–271.
(17) Aspnes, D. E. *J. Opt. Soc. Am. A* **2004**, *21* (3), 403–410.
(18) Herzinger, C. M.; Johs, B.; Mcgahan, W. A.; Woollam, J. A.; Paulson, W. *J. Appl. Phys.* **1998**, *83* (6), 3323–3336.
(19) Nielsen, L. E. *J. Phys. D: Appl. Phys.* **1974**, *7* (11), 1549–1554.
(20) Johs, B.; Herzinger, C. M. *Thin Solid Films* **2004**, *455*−*456*, 66–71.
(21) Certain commercial equipment and materials are identified in this paper in order to specify adequately the experimental procedure. In no case does such identification imply recommendations by the National Institute of Standards and Technology nor does it imply that the material or equipment identified is necessarily the best available for this purpose.